Journal of Advances in Science and Technology
Vol. 21, Issue No. 2, September-2024, ISSN 2230-9659

DOI: https://doi.org/10.29070/b4jcxd80

A Study of Gravity Wave Characteristics at High Frequencies

Vikash Kumar Singh [1] * , Dr. Arvind Kumar [2]

1. Research Scholar, Shri Krishna University, Chhatarpur, M.P., India
vikashami92@gmail.com ,
2. Associate Professor, Shri Krishna University, Chhatarpur, M.P., India

Abstract: Atmospheric dynamics rely heavily on gravity waves (GWs) because of their effects on turbulence formation, energy and momentum transmission, and the thermal structure of the middle atmosphere as a whole. Using data from COSMIC GPS RO satellites and high-resolution radiosonde measurements, this research examines the properties of high-frequency gravity waves. This research finds major vertical wavelengths and their seasonal changes by analysing wind and temperature fluctuations throughout various seasons and altitudes. The findings show that there are consistent patterns of propagation for high-frequency GWs with vertical wavelengths in the troposphere ranging from 6-12 km and in the lower stratosphere from 3-7 km. In the troposphere, horizontal wavelengths are 100–300 km, and in the lower stratosphere, they may reach 500 km. Additionally, convection is seen as a possible driving element when looking at these waves from a global viewpoint. Improved atmospheric modelling and climate projections are aided by the study's results, which add to a better understanding of GW dynamics.

Keywords: Troposphere, GW dynamics, Atmospheric Dynamics, Climate, Satellites

X

INTRODUCTION

In view of the far-reaching effects that they have on the structure and dynamics of the atmosphere, gravity waves (GWs) have become a central focus of research in the field of contemporary atmospheric science. There have been a great number of theoretical, computational, and observational investigations that have demonstrated that gravity waves play a significant role in the transfer of energy and momentum, the generation of turbulence, as well as the mixing, regulation, and impact on the thermal structure and mean circulation of the middle atmosphere. [1]

By parameterizing gravity wave drag, it is possible to generate accurate simulations of the middle atmospheric circulation using large-scale numerical models, as shown by research. This is important in order to get the desired results. In order to do this parameterization, it is necessary to have parameters that correspond to wave qualities. [2] These parameters may be determined by observations. Studying the climatology of global warmings (GWs), which must take into account their whole spectrum, is necessary in order to get a comprehensive understanding of the influence that GWs have on atmospheric phenomena. Research that examines different time periods is scarce in tropical locations, in particular.[3]

This is especially true for tropical tropical settings. [4] On a more specific level, the primary explanation is that there are not enough viable experimental procedures that have high enough spatial and temporal resolutions. Radiosonde data are used widely in the field of global warming research because to the vast geographical coverage they provide. In spite of the fact that they are helpful for researching long-period

GWs in the inertial area, the temporal resolution of these models is a disadvantage. [5]

Since the emergence of VHF/UHF radars, which offer three-dimensional winds with tremendous spatial and temporal resolutions, we have made significant progress in defining these GWs. This has allowed us to describe them in more detail. It is possible to make a comparison between the outcomes of VHF radar experiments and the many GW spectral models that have been developed. [6]

There have been a lot of studies that have used radiosonde observations in order to extract GW low frequency components up to this time. On the other hand, the characteristics of high-frequency GW as seen by radiosondes have been the topic of a very small number of study. Geller and Gong (2010) were the first people to extract the parameters of high frequency GW components from radiosonde ascent rates. This was a significant achievement. This chapter illustrates, for the very first time, that high frequency GWs may be analyzed by using high resolution radiosonde observations of wind and temperature. This is accomplished by applying the well-known least square fitting technique.[7]

It is possible to extract the durations of these GWs by using the simultaneous data received from the MST radar. Due to the fact that the network of radiosondes was unable to produce a worldwide picture of these waves, the data from GPS RO satellites were used. Five years' worth of COSMIC GPS RO temperature profiles have been evaluated using a method that is quite comparable. The altitude range that was studied was between 18 and 35 kilometres. [8]

RESEARCH METHODOLOGY

The background mean vertical structure must be removed from the individual wind and temperature profiles before the GW characteristics can be extracted. This is a prerequisite for the extraction of the GW characteristics. In the present study, the seasonal mean profile was removed in order to get the fluctuation components in the zonal wind (U), the meridional wind (V), and the temperature (T). The four different seasons are winter (December–February), pre-monsoon (March–May), monsoon (June–August), and post-monsoon (September–November). Winter occurs between the months of December and February.

Linear interpolation is used to fill in the sparse data gaps that occur during a season. This is due to the fact that balloons are only capable of traveling up to 30 kilometers. Due to the fact that the inertial period linked with Chhatarpur (13.5oN) is less than 52 hours, a high pass filter with a cutoff of three days was used in order to exclude the impact of waves that have durations that are greater than 52 hours. Inertial gravitational waves (GWs) and tides are two factors that contribute to the fluctuation profiles that have been documented. In later sections, we shall illustrate how they are distinct from HGWs, which are another name for high frequency gravity waves. From the filtered (U', V', and T') radiosonde data, the least squares method was used in order to derive the vertical wavelength that was the most dominant for each day's profile.

Due to the fact that the Brunt Vaisala frequencies fluctuated between 0 and 16 kilometers in the troposphere and 16 and 28 kilometers in the stratosphere, it was necessary to use the least square fitting method for the vertical wavelength of each area. It is important to keep in mind that this separation is only applicable to this station; when it is used in other latitudes, the level of care that is required will be determined by the height of the tropopause. Complying with the criterion of having the largest amplitude

and the lowest RMS deviation is necessary in order to locate the dominant vertical wavelength. As an example of the method, a sample situation is shown in Figure.

It is important to keep in mind that the most prominent vertical wavelengths, with the biggest amplitude and the lowest root-mean-square deviation, correspond to 11 kilometers and 5.6 kilometers, respectively, when the least square method is done between 0 and 16 kilometers and between 16 and 28 kilometers, respectively. Another conspicuous vertical wavelength may be seen in the troposphere at a distance of about 5.2 kilometers. Considering that wavelengths in the troposphere that are shorter than 5 kilometers in length could be connected with inertial period G, this study does not take them into consideration.

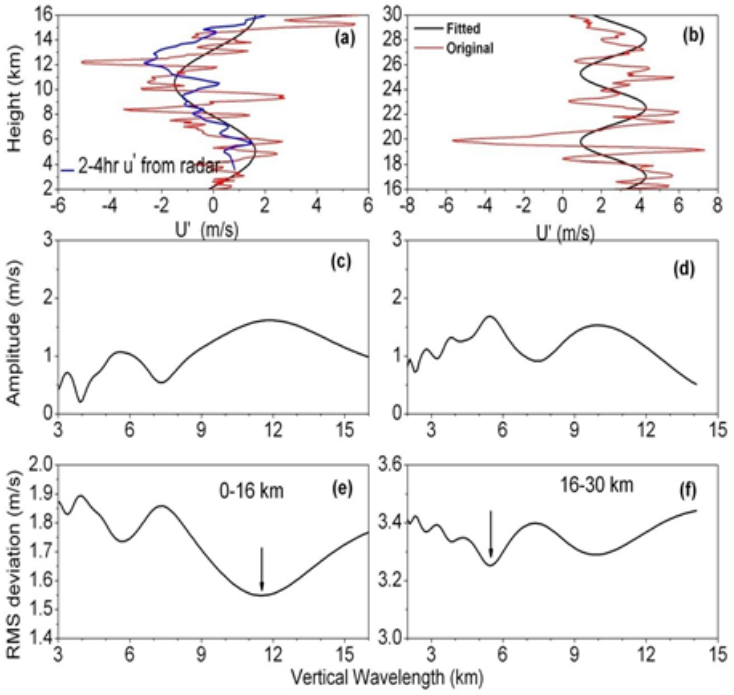

Figure 1: On 15 January 2021, radiosonde observations in the troposphere and lower stratosphere revealed typical profiles of zonal wind variations (redline) and their best fits (black line), illustrating the main vertical wavelength using the least square approach. Additionally, the panel(a) displays the overlay (blue line) 2-4h filtered fluctuation profile acquired from MST radar.For the troposphere, the amplitude and root-mean-square deviation were shown in (c) and (d), while for the lower stratosphere, they were presented in (e) and (f).

RESULTS

Spectrum in the vertical plane

The analytical method that was mentioned above was used to all of the radiosonde data over the last five years (May 2017–April 2022) in order to differentiate between the troposphere (0–16 km) and the lower stratosphere (16–28 km) and to identify the vertical wavelengths that make up the majority of each of these regions in U, V, and T. According to what was said before, the study in question takes into consideration the dominant vertical wavelengths in the troposphere that have values of 5.5 kilometers or more. The figure

presents the percentage of times that the dominant vertical wavelengths occurred between May 2017 and April 2022, as measured separately in U, V, and T. This information may be found in the figure.

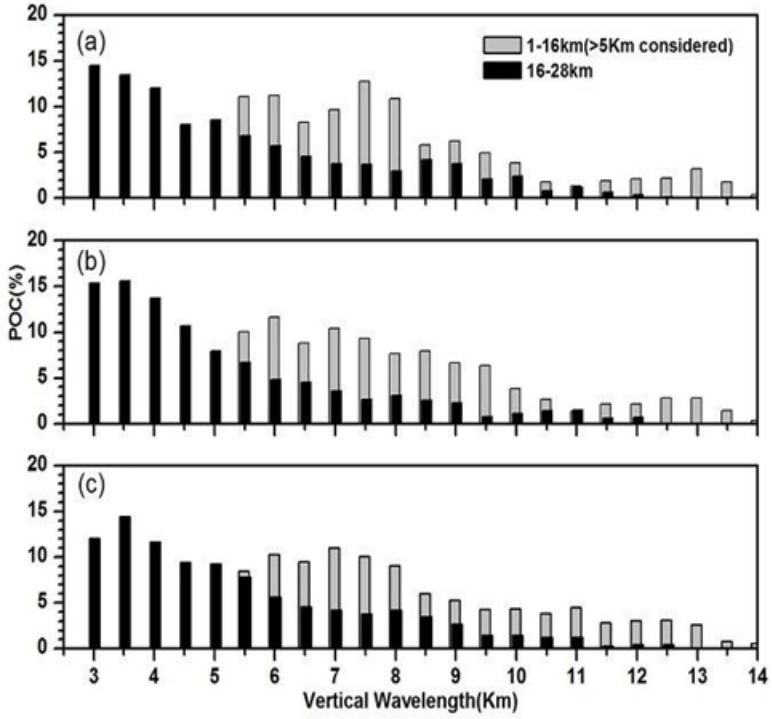

Figure 2: In this histogram, the most notable vertical wavelengths in the zonal wind, the meridional wind, and the temperature data gathered from radiosonde observations over Chhatarpur from May 2017 to April 2022 are shown. These measurements were taken from about the same time period. Here, we can observe the lower stratosphere, which is represented by black bars spanning from 16 to 28 kilometers, and the troposphere, which is represented by gray bars ranging from 1 to 16 kilometers

Table 1: Frequency distribution of seven distinct examples in the 1-16 km and 16-28 km vertical wavelength ranges (in brackets)

Seasons	Vertical wavelength range(km)	In all u, v and t	Only u not in v and t	Only v not in u and t	Only t not n u and v	Only in u and v not t	Only in u and t not v	Only in v and t not u
Monsoon	5.5-7.5 **(2.5-4.5)**	1.3 (7.2)	29.6 (20)	29.9 (28.2)	33.5 (24.5)	3.9 (10. 7)	4.9(6.9)	3.7 (5.1)
	7.5-10.5 **(4.5-7.5)**	0 (1.7)	21.1 (16.8)	24.5 (19.7)	18.2 (18.7)	1.8 (2.1)	1.3 (4.8)	3.1 (2.4)
	10.5-13.5 **(7.5-10.5)**	0.3 (0.8)	9 (12.7)	7.9 (5.1)	13.7(10.4)	0.5 (0.3)	0.8 (1.6)	0.5 (1.1)
	13.5-16.5 **(10.5-13.5**	0 (0)	0.8 (1.9)	2.1 (1.3)	0 (2.4)	0 (0)	0 (0)	0 (0.27)
Post Monsoon	5.5-7.5 **(2.5-4.5)**	2.3 (6.5)	31.4 (17)	30.1 (26.7)	25.7 (24.3)	4.6 (10)	4.1 (7.8)	5.9 (7.5)
	7.5-10.5 **(4.5-7.5)**	0 (0.5)	19.4 (18.9)	20.7 (17.3)	22.4 (22.1)	1.7 (1.6)	4.1 (1.9)	2.6 (1.6)
	10.5-13.5 **(7.5-10.5)**	0 (0)	5.1 (11.6)	9.7 (7.5)	13.0 (9.4)	0.3 (1.3)	0.8 (1.9)	0.26 (0.27)
	13.5-16.5 **(10.5-13.5)**	0 (0)	0.77 (2.7)	1.8 (2.4)	0 (1.9)	0(0)	0(0)	0 (0)
Winter	5.5-7.5 **(2.5-4.5)**	0.3 (3.9)	28.8 (23.6)	25.6 (30.4)	29.1 (24.8)	4.8 (7.0)	4.5 (4.2)	2.1 (5.9)
	7.5-10.5 **(4.5-7.5)**	0.3 (0.3)	21.9 (23.9)	22.1 (18.6)	24.8 (26.8)	3.4 (1.7)	1.1 (3.1)	1.9 (4.2)
	10.5-13.5 **(7.5-10.5)**	0 (0.6)	10.1 (12.9)	9.9 (11.5)	15.2 (8.2)	1.1 (0.28)	0.5 (0.8)	0 (0.8)
	13.5-16.5 **(10.5-13.5)**	0 (0)	0.5 (1.7)	1.1 (3.1)	0.5 (2.5)	0 (0)	0 (0)	0 (0)
Pre monsoon	5.5-7.5 **(2.5-4.5)**	0.6 (3.5)	27.6 (22.8)	28.2 (28.6)	30.2 (24.9)	7.69 (9.4)	8.5 (6.1)	5.4 (6.7)
	7.5-10.5 **(4.5-7.5)**	0 (0)	20.5 (24)	20.2 (22.2)	19.1 (26.6)	0.85 (4.4)	1.9 (3.8)	4.3 (2.9)
	10.5-13.5 **(7.5-10.5)**	0 (0.6)	9.1 (8.2)	7.9 (7.3)	8.3 (11.1)	0.3 (0.6)	0.8 (0.6)	0 (0.9)
	13.5-16.5 **(10.5-13.5)**	0 (0)	0.9 (1.5)	1.1 (2.6)	1.7 (1.6)	0 (0)	0 (0)	0 (0)

In the vicinity of the troposphere, a total of 1520 launches were carried out during the months of May 2017 and April 2022. There were 1151 observed vertical wave lengths in the zonal wind that were more than 5 kilometers, 1163 discovered in the meridional wind, and 1219 detected in the temperature. In the stratosphere's zonal wind, meridional wind, and temperature, respectively, launches at 1215, 1247, and 1252 MHz exhibited vertical wavelengths that were more than 2.5 kilometers.

Vertical wavelengths of up to 14 kilometers are seen in all three measurements, but those of more than 10 kilometers and 5 kilometers are very uncommon in the troposphere and lower stratosphere, respectively. While it is true that all three measurements display longer vertical wavelengths on any given day, it is important to note that they do not do this simultaneously.

The following is a list of the four ranges of vertical wavelengths in U, V, and T that will be used in order to conduct an in-depth examination of this feature: the range for the troposphere is between 2 and 4.5 kilometers; the range for the stratosphere is between 4.5 and 7.5 kilometers; the range for both is between 7.5 and 10.5 kilometers; and the range for both is between 10.5 and 13.5 kilometers. It is feasible to calculate the proportion of vertical wavelengths for each of the seven different scenarios by using the following formula: instance 1, in which the same vertical wavelength is present in all three parameters U, V, and T; instance 2, in which it is present in U and V but not in T; instance 3, in which it is present in U but not in V; instance 4, in which it is present in V but not in U; instance 5, in which it is present in U but not in V and T; instance 6, in which it is present in V but not in U and T; and finally, instance 7, in which it is not present in either of these parameters U or V.

In Table , we are able to see the seasonal distribution of the proportion of these seven circumstances over a variety of wavelength ranges. It is observed that the proportion of high vertical wavelengths increases in proportion to the wavelength range, in contrast to the usual features. A further point to consider is that the frequency of vertical wavelengths does not fluctuate much throughout the year.

Periods of a wave

These higher vertical wavelength waves have been found utilizing MST radar data for a period of 72 hours during the SAFAR intensive campaign period, as was previously mentioned. These periods correlate to the waves that have a higher vertical wavelength. It is important to keep in mind that separate radiosonde readings taken every six hours are used in order to get the vertical wavelengths. We were successful in extracting comparable dominant periods from 12-hour MST radar data by using the least square fitting technique in the time domain.

As an illustration of a typical example of the least square model, the data that was collected between the 15th and 16th of January 2010 at an altitude of 13 kilometers for the time series of U, V, and W is shown in Figure. The amplitudes of all three measurements, with the exception of the root-mean-square (RMS) measure, are at their highest between two and four hours apart. On the other hand, the U component experiences a second dominant phase between the hours of 7 and 9, the V component between the hours of 4 and 6, and the W component between the hours of 4 and 5.

It is necessary to make use of a band pass filter that has a pass range of between two and four hours in order to further optimize these three characteristics. Those panels at the bottom of the figure display the

filtered data that was produced as a consequence. By applying least square fitting to these perturbations at different altitudes, a dominant vertical wavelength of 10–11 kilometers is produced. This vertical wavelength matches the vertical wavelength produced by the corresponding radiosonde observations, demonstrating that the higher vertical wavelengths correspond to intervals of 2-4 hours.

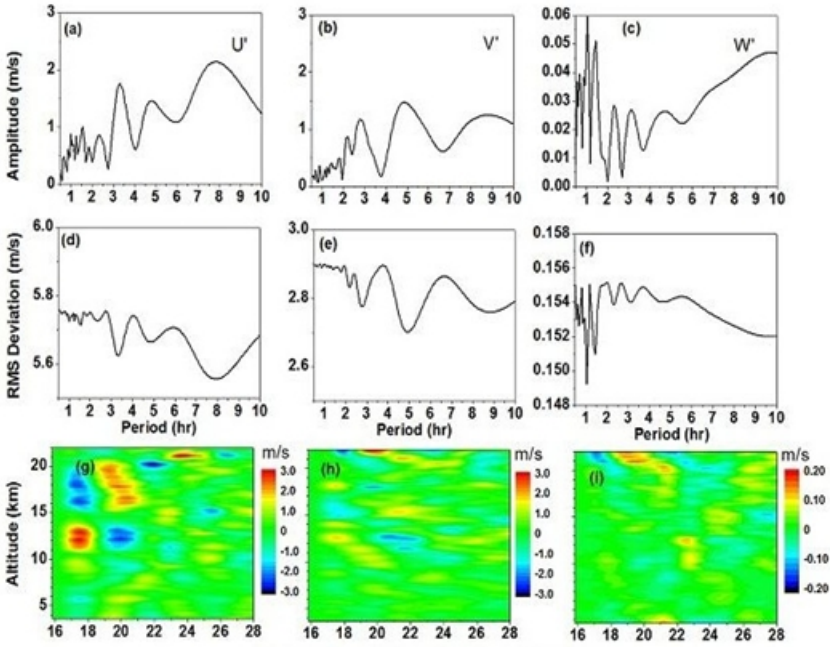

Figure 3: For the Indian MST radar data collected between January 15th and 16th, 2021, the amplitude and root-mean-square deviation reveal the dominating periods as determined by the time domain application of the least-square fitting technique. Variations in zonal, meridional, and vertical winds are shown on contours after the use of a 2-4 hour band pass filter

Using the same methodology, we examine all campaign data from 2008 to 2010 and find that the longer vertical wavelengths are associated with waves that last between two and six hours. This lends credence to the idea that radiosonde data alone may be used to derive GW features at high frequencies (vertical wavelengths).

Wavelength in vertical direction

Now that we have the periods and vertical wavelengths of the high frequency GWs, we can use the applicable dispersion relation to derive the horizontal wavelengths. Here is the dispersion relation for gravity waves at high frequencies:

$$\omega^2 = N^2(k^2 + l^2)/m^2$$

This is where the variables m stands for the vertical wave number, ü for the period, k and l for the zonal and meridional wavenumbers, respectively, and N for the Brunt Väisälä frequency, which is calculated independently for the troposphere and lower stratosphere from individual radiosonde readings. By combining the vertical wavenumber derived from radiosonde data with the periods derived from MST radar data, one may determine the horizontal wavelength, also called the wave number.

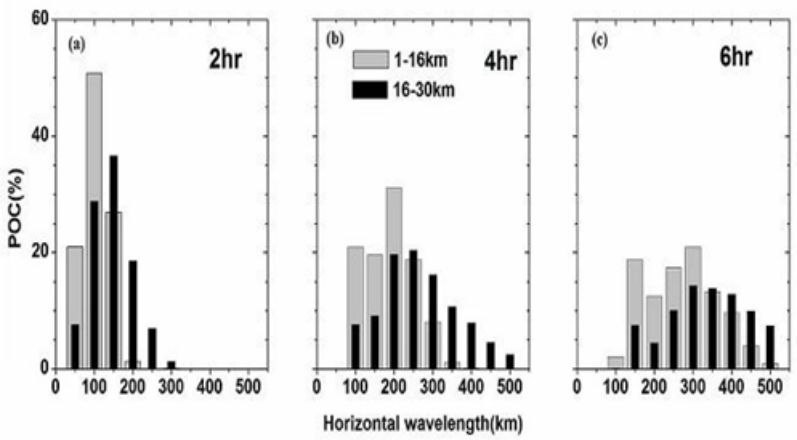

Figure 4: For various wave periods, histograms displaying horizontal wavelengths in the troposphere (gray bars, 1-16 km) and lower stratosphere (black bars, 16-28 km) are shown as percentages.

The horizontal wavelengths that were found to be the most dominant across all of the aforementioned time periods were found to be between 100 and 300 kilometers in the troposphere and up to 500 kilometers in the lower stratosphere on average. Compared to the horizontal wavelengths that were previously reported for GWs with an inertial period (Sasi et al., 2000), these horizontal wavelengths are much shorter. They are in agreement with the findings that were obtained by Dutta et al. (2009) for waves that have a short period of less than two hours. This equation may be viewed to reflect the intrinsic frequency, which is denoted by the symbol π. After doing the hodograph study, which will be covered in the next section, it was determined that the inherent frequency of the waves that were seen is pretty close to the frequency that was displaced by the Doppler effect. If Doppler-shifted periods are used in Equation , then the horizontal wavelengths that are predicted may not be too far off from the actual values.

Propagation in a horizontal direction

The hodograph analysis that was conducted to the radiosonde data was used to estimate the horizontal propagation direction of the GWs that were identified. As a result of the polarization relation of GWs, it is possible to deduce that propagation occurs along the principal axis of the horizontal wind vector hodograph. However, the temperature gradients that follow the phenomenon give the specific direction in which the phenomenon is propagating. An extensive amount of study has shown that it is not usually the case that all three qualities display big vertical wavelengths at their same moment. Hodograph analysis is used in order to determine the equivalent amplitudes in V and T. This is accomplished by referring to the vertical wavelength that is dominant in U.

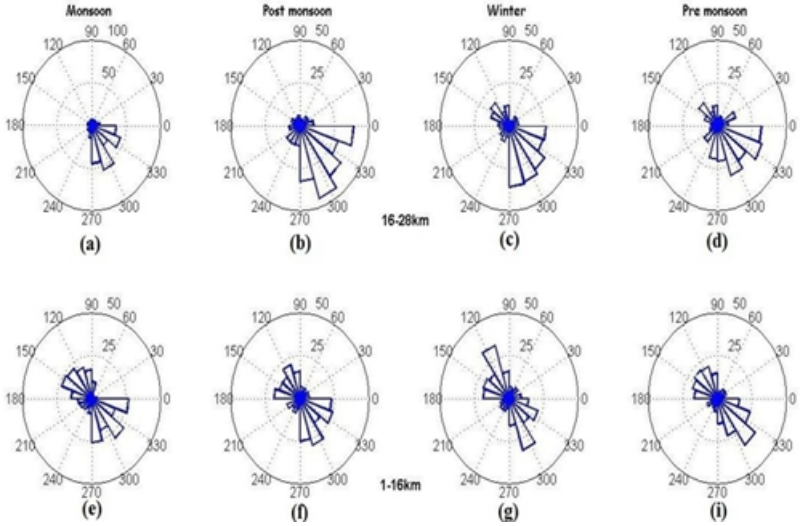

Figure 5: Various seasons from May 2017 to April 2022, the horizontal direction of gravity wave propagation (in percentage terms) sorted every 30 degrees in the lower stratosphere (16-28 km, top row) and troposphere (1-16 km, bottom row) areas. The directions indicated by the values 0o, 90o, 180o, and 270o are eastward, northward, westward, and southerly, respectively. Except during the monsoon season in the stratosphere, the inner and outer rings are drawn at 25% and 50% occurrences, respectively

Furthermore, it has been shown that the two directions of horizontal propagation are similar by using V as a point of reference via the use of measurements. Through the use of U as a point of reference, the figure illustrates the horizontal propagation direction of GWs that were estimated separately for the troposphere and lower stratosphere of the atmosphere throughout different seasons. In the lower stratosphere, the predominant horizontal propagation direction is south-east, but in the troposphere, it is north-west/south-east. This is made abundantly evident by the image. It would seem that the background wind is responsible for filtering out waves that propagate in the north-west direction in the troposphere before they reach the stratosphere. This is an unexpected finding considering that it is often assumed that GWs begin in the troposphere. It is during the monsoon season that this filtering becomes starkly obvious, despite the fact that the upper troposphere is subject to a strong easterly background wind.

The world as seen via high-frequency gravity waves

In order to get a global picture of these waves, we relied on data from GPS RO satellites since the network of radiosondes provides inadequate information. In the region ranging from 18 to 35 kilometers in height, the COSMIC GPS RO temperature profiles over a period of five years have been studied using the same methodology. As a result of the fact that the research was carried out between 18 and 35 kilometers, the maximum vertical wavelength that has been found will be 17 kilometers. According to what was said before, the wavelength in the troposphere will be twice as long as the wavelength in the stratosphere. The previous research that used radiosonde data demonstrated that the range of these high-frequency waves is between three and eight kilometers when they are at an altitude of sixteen to twenty-eight kilometers. In light of this, we have divided them into four bands: 2-4, 4-6, 6-8, and 8-10 kilometers, so that you can see the vertical wavelength's dominant range.

Figure demonstrates that the bulk of the data can be classified into two distinct bands: 4-6 kilometers and 6-8 kilometers. There was a high degree of concordance between the readings taken by the radiosonde and this particular range of wavelengths. Additionally, it is the most noticeable of the two between the values of 200S and 200N. A lower than 230 W/m OLR Given that these two layers are stacked on top of one another, it is reasonable to assume that convection is a possible contributor to the high-frequency waves that are encountered. Researchers examined each of the four seasons separately throughout the course of the whole five years, from 2017 to 2022 (figures are not shown), and their results suggested that the vertical wavelength range of the tropical high-frequency waves was between 4 and 8 kilometers.

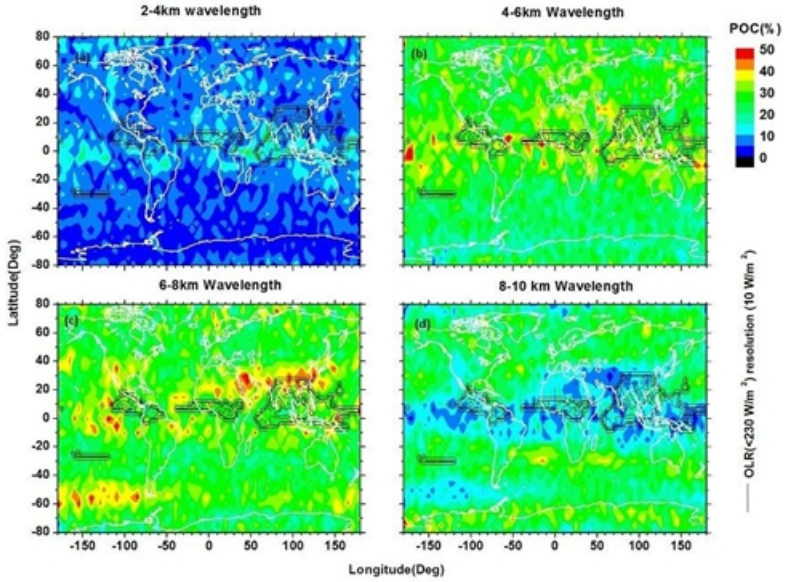

Figure 6: From 2017 to 2022, the frequency of various vertical wavelength bands, overlaid with an OLR < 230 W/m 2, was measured between 18 and 35 km

A number of studies have been conducted in the past that have used data acquired from radiosondes in order to investigate low frequency GW characteristics. An method called as least square fitting was used for the very first time in order to extract high-frequency GW characteristics. This was accomplished by making use of high resolution radiosonde data that has been accessible from the tropical station Chhatarpur since May of 2017. In the beginning, the vertical wave lengths are obtained by first taking the profiles of the troposphere and the lower stratosphere separately.

Vertical wavelengths in the troposphere and lower stratosphere, which are, respectively, 6-12 kilometers and 3-7 kilometers, been seen on several occasions and do not exhibit any seasonal predilection either. By using simultaneous MST radar data, it has been found that these waves with a longer vertical wavelength correspond to GW durations that range from two to six hours. According to the dispersion relation, the horizontal wavelengths of the troposphere range from 100 to 300 kilometers, but the lower stratosphere may have wavelengths that are as high as around 500 kilometers.

Global warming tends to extend horizontally in two ways: the troposphere, which faces south-east and north-west, and the lower stratosphere, which faces south-east. Both of these directions are associated with the troposphere. In addition, the fact that a smaller percentage of occurrences of a single wavelength is

seen in all three components when compared to individual vertical wavelengths lends more credence to the notion that these waves are highly directed. In comparison to the inertial period GW that was published for the Chhatarpur site (Ratnam et al., 2008; Debashis Nath et al., 2009), the characteristics that are being discussed here are different. Regarding the vertical wavelengths of IGWs at the Chhatarpur site, the present research does not take into consideration the fact that these wavelengths are in the range of three to five kilometers.

Additionally, a global picture of these frequency waves has been reconstructed from the data that was carried back by spacecraft. It is easy to see that the primary vertical wavelength range of these waves is between 4 and 8 kilometers at an altitude between 18 and 35 kilometers. The lower OLR values indicated that convection might be a viable source of wave generation, which is consistent with both theory and practice. The work that is being done will be beneficial to the parameterization of these components in the global models.

In this chapter, it is made abundantly clear that a radiosonde may be used to investigate high-frequency gravity waves that occur between two and six hours. It is well knowledge that tides, which are analogous to these gravity waves, possess a substantial role in the middle atmosphere as well.

CONCLUSION

Insights into high-frequency gravity waves have shown that they significantly alter the distribution of energy and the flow of air. Horizontal and vertical wavelengths, main propagation directions, and seasonal fluctuations are among the important wave properties that the research correctly finds. The findings point to the presence of two main horizontal paths for high-frequency gravity waves: one in the lower stratosphere, running northwest to southeast, and another in the troposphere, running south to northwest. In addition, using data from satellites all across the world, the study proves that convective processes are directly responsible for wave creation. In order to improve weather forecasting and climate simulations, our results highlight the significance of adding high-frequency GW features to atmospheric models. To further comprehend the function of gravity waves in atmospheric dynamics, future studies should aim to enhance numerical modelling and hone observational methods.

References

1. Bossert, K., Fritts, D. C., Pautet, P. D., Taylor, M. J., Williams, B. P., & Pendleton, W. R. (2021). Investigation of a mesospheric gravity wave ducting event using coordinated sodium lidar and Mesospheric Temperature Mapper measurements at ALOMAR, Norway (69°N). Journal of Geophysical Research, 119(16), 9765–9778. https://doi.org/10.1002/2014JD021460

2. Bossert, K., Kruse, C. G., Heale, C. J., Fritts, D. C., Williams, B. P., Snively, J. B., et al. (2017). Secondary gravity wave generation over New Zealand during the DEEPWAVE campaign. Journal of Geophysical Research: Atmospheres, 122(15), 7834–7850. https://doi.org/10.1002/2016JD026079

3. Cao, B., Heale, C. J., Guo, Y., Liu, A. Z., & Snively, J. B. (2016). Observation and modeling of gravity wave propagation through reflection and critical layers above Andes Lidar Observatory at Cerro Pachón,

Chile. Journal of Geophysical Research: Atmospheres, 121(21), 12750–12812. https://doi.org/10.1002/2016JD025173

4. Drob, D. P., Emmert, J. T., Meriwether, J. W., Makela, J. J., Doornbos, E., Conde, M., et al. (2019). An update to the Horizontal Wind Model (HWM): The quiet time thermosphere. Earth and Space Science, 2(7), 301–319. https://doi.org/10.1002/2014EA000089

5. Ejiri, M. K., Shiokawa, K., Ogawa, T., Igarashi, K., Nakamura, T., & Tsuda, T. (2023). Statistical study of short-period gravity waves in OH and OI nightglow images at two separated sites. Journal of Geophysical Research, 108(D21). https://doi.org/10.1029/2002JD002795

6. Geller, M. A., Alexander, M. J., Love, P. T., Bacmeister, J., Ern, M., Hertzog, A., et al. (2023). A comparison between gravity wave momentum fluxes in observations and climate models. Journal of Climate, 26(17), 6383–6405. https://doi.org/10.1175/JCLI-D-12-00545.1

7. Heale, C. J., Bossert, K., Vadas, S. L., Hoffmann, L., Dörnbrack, A., Stober, G., et al. (2020). Secondary gravity waves generated by breaking mountain waves over Europe. Journal of Geophysical Research: Atmospheres, 125(5), e2019JD031662. https://doi.org/10.1029/2019JD031662

8. Hecht, J. H., Kovalam, S., May, P. T., Mills, G., Vincent, R. A., Walterscheid, R. L., & Woithe, J. (2022). Airglow imager observations of atmospheric gravity waves at Alice springs and Adelaide, Australia during the Darwin area wave experiment (DAWEX). Journal of Geophysical Research, 109(D20), D20S05. https://doi.org/10.1029/2004JD004697